APPLICATION OF REMOTE SENSING AND GIS FOR FLOOD RISK ANALYSIS: A CASE STUDY AT KALU- GANGA RIVER, SRI LANKA

S.M.J.S.Samarasinghe[a] ,H.K.Nandalal[b], D.P.Weliwitiya[c], J.S.M.Fowze[d] , M.K.Hazarika[d], L.Samarakoon[d]

[a] GIS Branch, Survey Department, Sri Lanka.-(smjss265@yahoo.com), [b]Department of Civil Engineering, University of Peradeniya, Sri Lanka.-(h.nandalal@gmail.com), [c]Arthur C Clark Institute for Modern Technologies, Sri Lanka.-(dimuthprasad@yahoo.com), [d]GeoInformatics Center, Asian Institute of Technology, Thailand.-(jsmfowze, manzul, lal@ait.ac.th)

ABSTRACT:

Advances in remote sensing technology and new satellite platforms such as ALOS sensors widened the application of satellite data. One of the many fields that these technologies can be applied is to validate flood inundation models. For a long time flood extent from flood inundation models were validated using the ground truth surveys which was not very much reliable. In this study flood extent was extracted from satellite images available for one in 50 year flood event occurred on June 2008 in Kalu-Ganga River, Sri Lanka. Then that was compared with the flood extent derived from the flood extent obtained for the 50-year rainfall using HEC-HMS and HEC-RAS. Base on the flood extent, this project is to develop, demonstrate and validate an information system for flood forecasting, planning and management using remote sensing data with the help of Flood Hazard Maps for different return periods (10, 20, 50 and 100 years), Assess the population vulnerability and physical vulnerability of the lowest administrative division subjected to floods, and using above results conduct a flood risk analysis of the study area.

1. INTRODUCTION

Sri Lanka being located in the Indian Ocean between Bay of Bengal and Gulf of Mannar, pressure variations in the Bay of Bengal with high winds give rise to unexpected heavy rains. Further to that Sri Lanka experiences two monsoonal rains and two inter-monsoonal rains in a year. Due to these factors, lower reaches of rivers Kalu-Ganga, Kelani-Ganga and Gin-Ganga are subjected to frequent floods.

Ministry of Disaster Management was formed in 2006 and under its preview the Disaster Management Center (DMC) acts as the coordinating body of Disaster Release Managing (DRM) works in Sri Lanka. Since flooding is the most frequent natural disaster DMC has been focusing its attention to Flood Hazard Mapping as one of the priority tasks to be accomplished.

It is a question that the existing morphology of a river system can accommodate these frequent and prolonged high floods. The other question is the increasing human population encroaching and modifying the floodplains of river systems. All these factors contribute to the increasing damages and risks caused by floods. Due to the fertile flood plains and temperate climate that prevails in the Kalu-Ganga River basin it subjects to increasing human population encroachments which make the population more vulnerable to frequently occurring floods.

Those factors emphasis the importance of mitigating flood related disasters in Kalu-Ganga River. At present structural measures are not suitable in that task due to the question of sustainability of such measures. Most of the time non-structural measures like flood forecasting, proper early warnings and conducting awareness programs among the flood affected community etc., can be very effective. Modeling of watersheds with modern technology makes this easy. Application of GIS and remote sensing technology to map flood areas will make it easy to plan non structural measures which reduce the flood damages and risks involved. It will be a great benefit to the people to implement a flood management program that consists

of flood forecasting and flood hazard and vulnerability mapping. Therefore, benefits of this project are very much timely for the people living in the Kalu-Ganga river basin and governmental organizations to reduce flood risks in this area. This paper focuses on analyzing the flood risk in the lower reaches of the Kalu-Ganga River, in Kalutara District.

2. STUDY AREA

The study area is the Kalu-Ganga River basin in Sri Lanka. This river located in the western hill slopes of the island, which receives most of the south-west monsoon rainfall making the river basin vulnerable for frequent floods. Kalu-Ganga River watershed covers 2,658 km^2 and major land-use covers are forest, residential and agricultural cropland land use types.

Geographically the basin lies between the 6.32° and 6.90°N, and 79.90° and 80.75°E as per WGS84 coordinate system and flows from a height of about 2,250 m above MSL. (Figure 1)
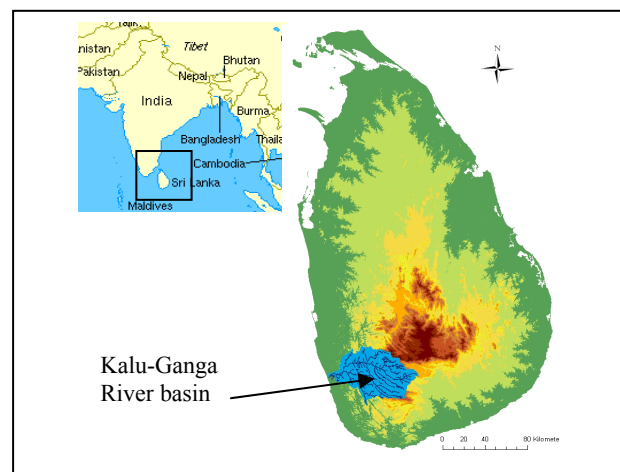

Figure 1: Kalu-Ganga River basin

3. DATA USED

3.1 Satellite Data

Henry et al. (2006) observed that polarization combination HH (horizontal polarizations in transmitting and receiving directions) provides a better discrimination of flooded areas than polarization combination HV or VV polarizations and several others like Wang et al. (2008) and Horritt (2006) used SAR images with HH polarization to detect floods. In this study also ALOS/PALSAR HH polarization was selected to detect flood extent. Satellite scenes were acquired during the dry season (March, 2008) as well as wet seasons (June, 2008) covering the study area.

3.2 Topographic and GIS Data

Topographic and GIS data used in this study consists of Digital Contour Maps, Spot Heights, Land use maps and LiDAR data. Contour maps used were in 1:10,000 scale with a contour interval of 5 m. The LiDAR data of the area are available only for a 2 km belt along the coastal line. Bathymetric cross section data of the Kalu-Ganga River was obtained from a survey project carried out by University of Peradeniya.

3.3 Hydro-Meteorological Data

Rainfall from 13 meteorological stations and stream flow data at 3 gauging stations were used. Discharges at three gauging stations from 1986 to 1996 were obtained from Department of Irrigation. Daily rainfall data of 13 rainfall gauging stations for the same period were obtained from the Department of Meteorology. These data were used to calibrate and verify the HEC-HMS model for the study area. Rainfall of 50 year return period for the Kalu-Ganga river basin was also obtained from the meteorological Department. Using a calibrated and verified HEC-HMS model for the basin discharges in the main river and tributaries corresponding to the rainfall of 50 year return period were estimated. Those are the input data for the HEC-RAS model that provides inundation areas.

3.4 Field Survey Data and Census Data

A questionnaire was designed and distributed among the people living in the flood plain and comments were collected. The N,E coordinates and the corresponding flood depths were quarried from the people. GN based population data collected from the Census Department.

4. METHODOLOGY

The methodology consists of data collection and data basing required for Hazard analysis and Vulnerability analysis. Based on the Hazard analysis and Vulnerability analysis, the Flood Risk analysis is carried out (Figure 2).
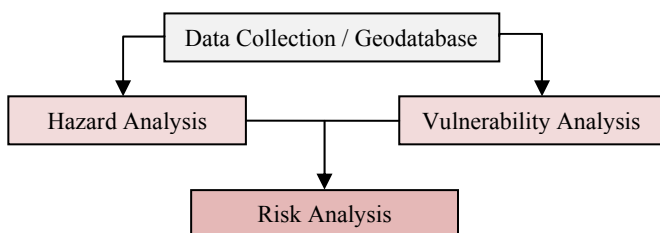

Figure 2: Methodology

Hazard analysis consists of Hydrologic/Hydraulic analysis, Topographical analysis and Satellite data analysis.
Vulnerability analysis consists of analyzing census data and outcome of the questionnaire survey to compute physical and social vulnerability.(Figure 2).

4.1 Hydrologic Analysis

Hydrologic analysis consists of application of HEC-HMS model. As availability of stream flow data was limited, a calibrated rainfall runoff model for the basin based on HEC-HMS was used to predict runoff for rainfall of 50 year return period.

Application of HEC-HMS (Hydrologic modeling software) that includes several hydrologic methods to simulate rainfall-runoff process in river basins. It consists of several models for calculation of losses and runoff due to a single rainfall event or a continuous rainfall.

To model rainfall runoff relationship for the basin, *HEC-HMS* was used. The basin model for HEC-HMS was prepared using Geospatial Hydrologic Modeling Extension *(HEC-Geo HMS)*, which uses ArcView and the Spatial Analyst extension of it. Using meteorological data, HEC-HMS model for the Kalu-Ganga River is developed. The model parameters were calibrated and verified on event basis using the rainfall runoff data available. Runoff data required for the HEC-RAS was computed using this calibrated and verified model.

4.2 Hydraulic Analysis

Application of HEC-RAS to obtain flood extent and depth. HEC-GeoRAS and HEC-RAS software were used.

HEC-GeoRAS is specifically designed to process geospatial data for use with the Hydrologic Engineering Center's River Analysis System (HEC-RAS). The tools allow users to pre and post process the data for HEC-RAS. It creates an input file for HEC-RAS containing geometric attribute data from an existing DTM and complementary data sets.

HEC-RAS is a 1D flow model in which the stream morphology is represented by a series of cross sections indexed by river station. Each cross section is defined by a series of lateral and elevation coordinates that are typically obtained from DTM. The flow chart of procedure to obtain the flood extent is explained in Figure 3.
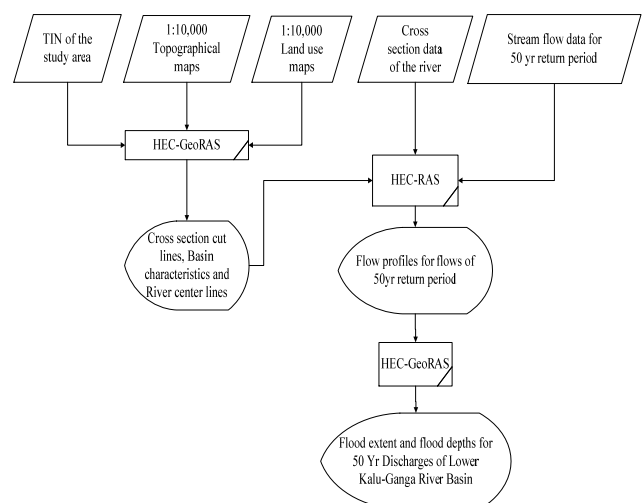

Figure 3: Steps applied for HEC-RAS modeling

4.2.1 Model Inputs

Implementation of HEC-RAS requires inputs which come from three basic categories of data; (i) Geometric data (ii) Basin characteristics and (iii) Flow data

Geometric Data

The requisite geometric data includes stream centerlines and cross section cut lines and these are prepared using the HEC-GeoRAS user interface. It is a set of procedures, tools, and utilities for processing geospatial data in ArcGIS. It also allows the import of the prepared data into HEC-RAS model. The creation of the import file requires a digital terrain model (DTM) of the river system. Having imported the data into the HEC-RAS system, the cross section data were adjusted to suit the available bathymetric profiles.

Basin Characteristics

Manning's friction coefficient 'n' falls under this category. The Manning's 'n' value is highly variable and depends on a number of factors including surface roughness, vegetation, channel irregularities, channel alignment, scour and deposition, obstructions, size and shape of the channel, stage and discharge, seasonal changes, suspended material and bed-load. Land-use map was used to extract the Manning's n value in this study.

Flow Data

Discharge and water level values make the upstream and downstream boundary conditions. For computing flood extent for rainfall of 50 year return period, flows computed using HEC-HMS was used as upstream boundary condition. The water level at river mouth is given as Sea water level (0m).

Flood Simulation

Having completed the set up of the system with the requisite model parameters and variables, a calibration run was performed using the peak discharge value corresponding to the 50 yr return period flood event. The initially used Manning's 'n' values were varied to give the downstream boundary condition. HEC-RAS model simulation results were exported to HEC-GeoRAS for further processing and visualization of flood extents. Results of this simulation are then checked against flood extent delineated from the satellite data which was at the scale of 50 year return period.

4.3 Topographical Data Analysis

The extraction of maps of the study area and development of the Triangular Irregular Networks (TIN) using contour maps, spot heights and LiDAR data were carried out. A geodatabase in Arc GIS environment was developed to the study area.

4.4 Satellite Data Analysis

The development of microwave remote sensing, particularly radar imageries, solve the problem. Apart from its all weather capability the most important advantage of using SAR imagery lies in its ability to sharply distinguish between land and water.

To detect flooded area in SAR imagery, it is generally performed by acquiring two imageries taken during a flood and during a dry time.

In the present study whole area of interest falls in two sets of satellite images. So they were mosaic together and cropped to extract the relevant area to analyze. First the images were filtered using Lee filter to reduce the noise.

To determine the threshold value the images were converted into decibel images (DB). Regions of Interest (ROI) were selected from both images which exhibit sharp changes in the pixel tone. After analyzing the statistics of ROI's a threshold value is determined from DB images to be used in image classification and masking. Using Band math operations the difference of these two images were calculated and masking was done according to the previously determined threshold value. Finally using the masking method the image was classified into two classes' flooded area and not flooded area. Finally flood extent derived from the ALOS/PALSAR image and the Flood Model HEC-RAS was compared. (Figure 4)
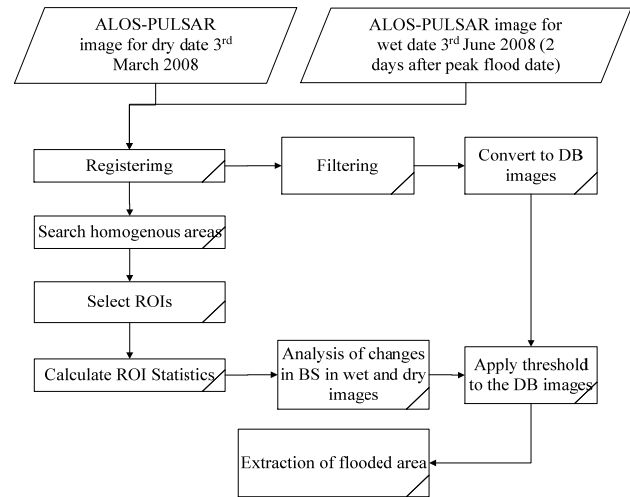

Figure 4: Methodology for flood extent delineation

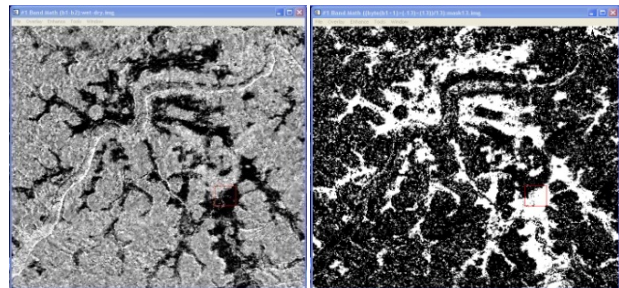Figure 5: ALOS PALSAR Images in Dry date and Wet Date.

Figure 6:   Figure 7:

Figure 6   - Image after performing the band math.
Figure 7   - Image after masking for flood areas.

4.5 Flood Hazard Mapping

Flood hazard is categorized based on the level of difficulties in daily life and/or damage to properties. Flood hazard assessment is the estimation of overall adverse effects of flooding. It depends on many parameters such as depth of flooding, duration of flooding, flood wave velocity and rate of rise of water level. One or more parameters can be considered in the hazard assessment. In the present study, depth of flooding was considered for hazard assessment. The intensity of flood hazard is always given by a relative scale, which represents the degree of hazard and is called a hazard rank. A smaller hazard rank was assigned for a lower depth or low hazard while larger hazard rank was used to indicate a higher hazard. (Table 1)

Depth (D) of flooding (m)	Hazard category	Hazard rank
Hazard free	No hazard	0
0<D≤1	Low	1
1<D≤3	Medium	2
3<D	High	3

Table 1. Hazard index for depth of flooding

Flood hazard maps for rainfall of 10, 20, 50 and 100 year return periods were developed.

4.6 Vulnerability Analysis.

Mainly two data sets were used for assessment of vulnerability of flood prone areas. First vulnerability was assessed for each GN division using population data and building data.
Secondly, a comprehensive household survey was conducted in the area of interest to collect data on the vulnerability of each household for flood.

4.6.1 Vulnerability Analysis with Census Data.

Vulnerability of all GN divisions was assessed using the age wise population data and construction materials used for the buildings. In the population vulnerability analysis, population of each GN division was categorized according to the age groups and assigned vulnerability rankings [$R(i)$] as in Table 2.

Category	Age Group	Ranking ,R(i)
1	Age < 5 Years	3
2	5 <Age <25 Years	2
3	25 <Age <60 Years	1
4	Age >60 Years	3

Table 2. Assignment of Ranks according to Age categories

Using the vulnerability ranking assigned to each age group, a population vulnerability index was calculated for each GN divisions from following formula.

$$PVI\ GN(i) = \sum_{(i=1\text{-}4)} FP\ GN(i)R(i) \qquad (1)$$

Where: **PVI GN(i):** The population vulnerability
FP GN(i) : Fraction of each age group
R(i) : Vulnerability ranking of each age group.

Category	Vulnerability index Range	Vulnerability Classification	Index
1	0.00 – 0.33	Low	1
2	0.33 – 0.66	Moderate	2
3	0.66 – 1.00	High	3

Table 3. Population Vulnerability Classification

Using the distribution of the vulnerability values a standardization procedure was carried out and GN divisions are classified as in Table 3.
This standardized vulnerability values were linked with the GN polygon map and it was overlaid with flood extent maps corresponding to 10, 20, 50 and 100 yr return period flood events. GN divisions which are not covered by flood are classified as Invulnerable GN divisions and their index value is changed to zero. In this way, population vulnerability maps were produced corresponding to 10, 20, 50 and 100 yr return period floods.
Following the same procedure, buildings (Physical) vulnerability indices of GN divisions were calculated. Only difference was that vulnerability rankings were assigned to each building category based on the material used.(Table 4)

Category	Construction Material	Ranking, R(i)
1	Brick	1
2	Kabok	3
3	Cement Blocks/ Stones	2
4	Pressed Soil Blocks	4
5	Mud	6
6	Cadjan / Palmyra	7
7	Planks/Metal Sheets	5

Table 4. Ranks according to Construction material

Following equation was used to calculate the vulnerability value of the GN divisions.

$$BVI\ GN(i) = \sum_{(i=1\text{-}7)} FB\ GN(i)R(i) \qquad (2)$$

Where: **BVI GN (i):** The Buildings(Physical) vulnerability of each GN division
FB GN (i): Fraction of the Buildings of each category
R(i) : Vulnerability ranking of buildings group.

Using the distribution of the vulnerability values, a standardization procedure was carried out and GN divisions are classified and the Building vulnerability maps were produced for each return period similar to the population.

4.6.2 Household Vulnerability Survey

Vulnerability can be defined as a function of contributing factors: exposure, sensitivity and adaptive capacity. Many more variables may also act as major contributing factors. However, from the previous vulnerability assessment done using population and building data. So in order to overcome this deficiency, a comprehensive household vulnerability survey was carried out to ascertain the total vulnerability of households in the region. Unlike the earlier vulnerability assessment, this survey incorporates many different factors to calculate the household vulnerability of each household.

Each of these contributing factors is then subdivided in to major component factors while they are also divided to sub component factors. The questionnaire was designed in such a way that each question is tied to a sub component. According to the answer given to a question a numerical value was assigned to each sub-component and its standardized index value [**Index (sHH)**] was calculated according to following equation.

$$Index\ (sHH) = (Shh - Smin)/(Smax - Smin) \qquad (3)$$

Where: **Shh** is the original sub-component value for the household,
Smin and **Smax** are the minimum and maximum values, respectively, for each sub- component determined using data from the household survey.

Using the sub-component values, major component values [**M(HH)**] are calculated. Then the major contributing factors are calculated utilizing following equation.

$$M(HH) = \sum\nolimits_{(i=1-n)} Index\ (sHH)i\ /\ n \qquad (4)$$

Where: **n** is the number of sub-components belonging to a major component.

These major component values were used to calculate the major contributing factor [**CF (HH)**] in terms of sensitivity, adaptive capacity and exposure. A weighting system (*Wi*) was introduced according to the relative importance of each major component within a certain contributing factor. (Table 5)

Major contributing factor	Major Components	Wi
Sensitivity	1. Demographic standing	4
	2. Land Characteristics	1
	3. Rural standing	2
	4. Water resources	3
Adaptive Capacity	1.Educational background	3
	2. Economic strength	1
	3. Assets	2
Exposure	1.Position relative to River	1
	2.Previous flood events	2

Table 5. Assigned weighting factors for major components

Considering the weighting factors assigned to major components contributing factors are calculated using following equation.

$$CF(HH) = [\ \sum\nolimits_{(i=1-n)} Wi\ M(HH)i\ ]\ /\ [\sum\nolimits_{(i=1-n)} Wi\ ] \qquad (5)$$

Where: **CF(HH)** is contributing factor (exposure, sensitivity, or adaptive capacity) for each household,
M(HH)i are the major components for Households,
Wi is the weight of each major component, a
n is the number of major components in each contributing factor.

Finally, contributing factors are used to calculate the Flood vulnerability index [**FVI**] of each household utilizing the following equation.

$$FVI = [E(HH)\ - A(HH)\ ]\ *\ S(HH) \qquad (6)$$

Where: **E(HH)** is the calculated exposure score,
A(HH) is the calculated adaptive capacity score,
S(HH) calculated sensitivity score for the household

Then considering the vulnerability distribution households were classified as shown in Table 6.

Category	Vulnerability Category	FVI Range
1	High	1.00-0.66
2	Moderate	0.66-0.33
3	Low	0.33-0.00

Table 6. Flood Vulnerability Classification

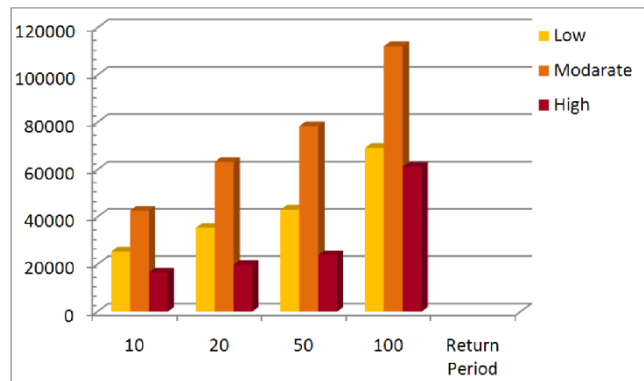**4.6.3 Results from Vulnerability Analysis**

Figure 8: Vulnerability of Population

Flood vulnerable maps for GN Divisions, Population and Household were produced according to rainfall of 10, 20, 50 and 100 year return periods in ARC GIS environment.

4.6.4 Results of Household Vulnerability Survey.

The vulnerability distribution of the households closely resembles a normal distribution. According to the distribution, most households had a vulnerability ranging from $0.3 - 0.6$ and they fall into moderate vulnerability category. The total number of households was 203.

Vulnerability Category	FVI Classes	Number of Houses
High	1 – 0.66	38
Moderate	0.66 – 0.33	150
Low	0.33 – 0.00	15

Table 7. Household vulnerability Statistics

4.7 Flood Risk Analysis

Considering risk as a function of Hazard & Vulnerability, map multiplication was done in ArcGis environment to generate the Risk Maps corresponding to 10, 20, 50 and 100 yr flood event with respect to both population and buildings.
It was assumed that:
 "Risk Index"= "Hazard index X Vulnerability index" and considering the risk index distribution, it was categorized in to 4 sets as in Table 8.

Category	Risk Value Range (m)	Risk Classification	Index
1	0 - 0	Risk Free	1
2	0 - 3	Low	2
3	3 - 6	Moderate	3
4	> 6	High	4

Table 8. Risk classification

4.7.1 Results from Flood Risk Analysis.

Flood risk analysis with respect to population revealed that approximately 11.3 km^2 area is under high risk category while 65.1 km^2 and 33.1 km^2 areas are under moderate and low risk categories respectively for the 100 yr return period flood.
Flood risk analysis with respect to buildings revealed that approximately 5.4 km^2 area is under high risk category while 45.8 km^2 and 58.3 km^2 areas are under moderate and low risk categories respectively in the 100 yr return period flood.
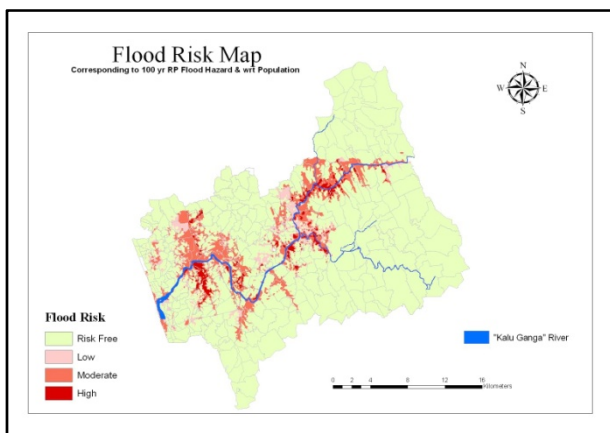Figure 9

Figure 9: Flood Risk Map for 100 Year period

5.0 RESULTS AND DISCUSSIONS

Flood extents derived from the satellite image satisfactorily matches that of the HEC-RAS model. The area near stream is dry according to the flood extent derived from satellite images. This can be expected as the images were taken on receding limb of the flood as flood peak had been occurred around two days before the satellite image was taken. However, the results are promising. The flood extents derived from the satellite image and the HEC-RAS matches very well though the extent was less in the satellite image.

6. 0 CONCLUSION

Remote sensing, GIS, and GPS together with flood modeling technique have successfully been applied to prepare the first ever set of Flood Risk Maps for the lower reach of the Kalu Ganga River-Sri Lanka in support of disaster preparedness and mitigation activities.
 For the first time in Sri Lanka ALOS/PALSAR derived remote sensing data was utilized successfully for extracting flood extent and thereby to calibrate/validate HEC-RAS model output.
 The study had produced a series of (10, 20, 50, 100 yr return period) Hazard maps followed by Vulnerability and Risk Maps corresponding to the above return period events and considering the vulnerability of population and buildings.
The study reveals that about 11.5 km^2 and 5.41 km^2 are at high risk with respect to population and buildings respectively for a 100yr return period flood event. Statistics for the moderate and low risks were found to be as follows; 65.5 and 46 km^2, and 33 and 58.5 km^2, respectively.
A household survey further revealed that approximately 19% of population is highly vulnerable for a 100yr return period flood event whilst the remaining 74% and 7% of them fall into moderate and low vulnerability classes, respectively.

REFERENCES

Brivio, P. A., Colombo, R., Maggi, M., Tomasoni, R., 2002. Integration of remote sensing data and GIS for accurate mapping of flooded areas. International Journal of Remote Sensing **23**(3), 429–441.
Chu, X., and Steinman, A., 2009. Event and Continuous Modeling with HEC_HMS. Journal of Irrigation and Drainage Engineering 135(1), 119-124.
HEC-GeoRAS, (2009) "Hydrologic Engineering Center's-*GeoRAS user's manual*, U.S. Army Corps of Engineers, Davis, Calif.(http://www.hec.usace.army.mil/software/hec-ras/hec-georas.html)
HEC-RAS, (2009) "Hydrologic Engineering Centers River Analysis System *user's manual*, U.S. Army Corps of Engineers, Davis, Calif.(http://www.hec.usace.army.mil/software/hec-ras)

Horritt, M.S., 2006. A methodology for the validation of uncertain flood inundation models. Journal of Hydrology 326, 153–165
Horritt, M.S., Bates, P.D., 2002. Evaluation of 1D and 2D numerical models for predicting river flood inundation. Journal of Hydrology 268, 87–99.

Islam, M.M., and & Sado, K., 2000. Development of flood hazard maps of Bangladesh using NOAA-AVHRR images with GIS. Hydrological Sciences Journal 45(3), 337-355

Mason, D.C., Bates, P.D., Dall' Amico, J.T., 2009. Calibration of uncertain flood inundation models using remotely sensed water levels. Journal of Hydrology 368, 224–236

Nandalal, H.K. and Ratnayake, U., 2009. Effect of Different Rainfalls on Kalu-Ganga River Runoff. Abstracts, Department of Natural Resources, Sabaragamuwa University of Sri Lanka, pp. 30.
Wang, Y. and Allen, T.R., 2008. Estuarine shoreline change detection using Japanese ALOS PALSAR HH and JERS-1 L-HH SAR data in the Albemarle-Pamlico Sounds, USA. International Journal of Remote Sensing, 29(15), 4429-4442.